Flexible and Printed Electronics

Process considerations for Aerosol-Jet printing of ultra fine features

To cite this article: Georg Gramlich *et al* 2023 *Flex. Print. Electron.* **8** 035002

Flexible and Printed Electronics

PAPER

Process considerations for Aerosol-Jet printing of ultra fine features

Georg Gramlich[1,*], Robert Huber[2], Florian Häslich[3], Akanksha Bhutani[1], Uli Lemmer[2] and Thomas Zwick[1]

[1] Karlsruhe Institute of Technology, Engesserstr. 5, 76131 Karlsruhe, Germany
[2] Karlsruhe Institute of Technology, Engesserstr. 13, 76131 Karlsruhe, Germany
[3] Fraunhofer Institute for Manufacturing Technology and Advanced Materials, Winterbergstrasse 28, 01277 Dresden, Germany
[*] Author to whom any correspondence should be addressed.

E-mail: georg.gramlich@kit.edu

Keywords: Aerosol-Jet, additive manufacturing, process optimization, printed electronics, high resolution

OPEN ACCESS

RECEIVED
15 April 2023

REVISED
26 June 2023

ACCEPTED FOR PUBLICATION
4 July 2023

PUBLISHED
20 July 2023

Abstract

In recent years, Aerosol-Jet (AJ) printing has become an increasingly popular technology applied in research ranging from the biomedical field to military applications to printed semiconductors. Extensive efforts have been made to understand the influence of process parameters and the underlying physical principles. Nevertheless, little attention has been paid to the optimization of ultra-small and highly precise printed features. Pushing the printer to its limits and manufacturing structures as small as tens of microns with a micrometer accuracy poses significant challenges, because effects that can be ignored for printing large features play a crucial role. This study demonstrates how the printing speed quickly causes intolerable distortions. In contrast to large-feature printing, the printing speed cannot be used as a free parameter to set the print thickness. We will discuss the non-constant printing behavior induced by the divert/boost shutter and present shutter on the fly as a solution to many problems, but only if the subroutine code is optimized. The modifications made to the code are disclosed in this paper for the first time. Knowing that printing precise features often results in a high print thickness, we will briefly discuss the issue of cracks caused by the drying of thick nanoparticle films. Altogether, this paper presents a range of important considerations for AJ printing ultra-fine features and an interesting insight into the particularities of operating the printer at its limits.

1. Introduction

Aerosol-Jet (AJ) printing is a non-contact manufacturing technology, which allows minimum feature sizes down to 10 μm. Most inks with a viscosity between 1 cp and 1000 cp can be utilized. Together with the available five-axis module, AJ printing is an extremely versatile process, which is of interest to many applications. It outperforms inkjet and screen printing in minimum feature size and supports a significantly wider range of inks than inkjet printers. Compared to UPD printing, the printing speed of an AJ printer is larger by orders of magnitude and it has the capacity to easily deposit onto non-planar surfaces. Researchers have hence put AJ printing to use in a multitude of fields ranging from medical applications [1, 2], over the preparation of active layers for polymer solar cells [3], to the development of fully printed carbon nanotube thin-film transistors [4]. AJ printing could additionally become an enabling technology in the field of radio frequency (RF) electronics: Recent advances in semiconductor technology enable monolithic microwave integrated circuits (MMICs) with operating frequencies in the THz range. Connecting the RF signal of an MMIC to a printed circuit board poses a hitherto unsolved challenge if high performance, broadband behavior, and an economical manufacturing cost are to be achieved. AJ-printed silver interconnects are a promising solution for this packaging bottleneck as the current research proves: The first AJ-printed MMIC interconnects have been published, which operate up

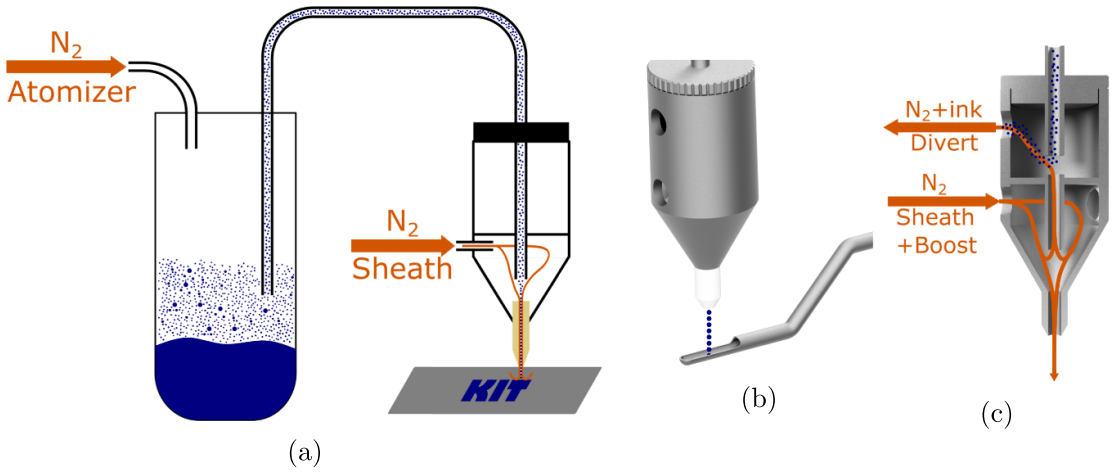

Figure 1. (a) AJ working principle. (b) Working principle of the mechanical shutter. (c) Working principle and gas flows of the divert/boost shutter.

to 20 GHz [5], 60 GHz [6], 67 GHz [7], 92 GHz [8], and even 200 GHz [9].

A wide variety of THz applications require very precise printing of small structures, low surface roughness, and high conductivity. The higher the operating frequency is, the more pressing these requirements become. In our own work on printed AJ millimeter-wave circuitry [10] and packages [11], we have collected experience on AJ printing process optimization for structures with minimum feature sizes down to 20 μm. They require a dimensional accuracy of at least 5 μm. Considering that AJ printing is commonly used to print mm to cm large structures, features between 10 and 200 μm will be called ultra-fine from here on and a dimensional accuracy better than 20 μm will be referred to as highly precise. Any structure sizes above those will in consequence be denominated 'large feature' for the rest of this article. To the best of our knowledge, this is the first published analysis of process considerations for AJ printing ultra-fine and highly precise features. We will discuss how effects, which can be ignored for printing large features, become relevant for highly precise applications with small features. The problems these effects cause will be discussed and we will show how to solve them. The paper begins with a brief discussion of the AJ working principle. This is followed by the influence of the printing speed and by the properties of the divert/boost shutter. Shutter on the fly (SOTF) will be presented as an excellent solution and we will disclose our improved subroutine code. The paper will end with a discussion of how drying ink can lead to cracks in thick printouts and how to avoid them. We believe that the novel contributions of this paper will be helpful in many fields of application where researchers want to manufacture ultra-small features using AJ printing.

1.1. AJ working principle

AJ printing is a contactless additive manufacturing technology, that allows printing structures down to 10 μm size. The raw material needs to be presented as an ink with a viscosity between 1 and 1000 cp. This ink is subsequently atomized into an aerosol, which is then filtered to achieve a homogeneous droplet size. In the next step, the aerosol is transported to the printing nozzle. This gas stream is called the atomizer flow. In the nozzle, a sheath gas stream is wrapped around the atomizer flow, which results in a focusing effect and shields the nozzle from the droplets at the same time. This gas stream is called the sheath flow. Figure 1(a) gives an overview of the working principle and of the most important gas streams. The printhead or the substrate can be moved to print lines, and printing adjacent lines allows to create surfaces. The AJ5X AJ printer by Optomec, which has been used to perform all experiments shown in this work, has two different shutter mechanisms. The first option is to interrupt the gas stream that leaves the nozzle with a mechanical shutter, see figure 1(b). This mechanism consists of a spoon that is moved between nozzle and substrate and thereby stops the printing. This mechanism has an extremely fast response time of approximately 5 ms but comes with the disadvantage that the spoon can fill up and cause ink splashes. The second shutter mechanism is called the divert/boost shutter. It leads the atomizer gas stream with the aerosol into a filter and replaces it with a dry nitrogen gas stream called boost, that keeps the pressure in the nozzle constant, see figure 1(c). Additionally, a part of the boost flow is moving upwards through the nozzle and eventually sucked out by the divert flow as well. This upwards running gas stream efficiently prevents any aerosol droplets from leaking. The obvious advantage of the divert/boost shutter is that there is no spoon

that could fill up and cause splashes but the response time is also significantly slower, around 100 ms, and for very small atomizer flow rates a non-constant printing behavior can be observed after turning the shutter off for an extended time, as will be shown later. A detailed explanation of the working principle of AJ printers is given in [12], and Secor describes in [13] how the atomizer and sheath gas streams influence the line geometry based on fluid dynamics. A thorough investigation of overspray is presented in [14]. Mahajan *et al* [15] published an experimental investigation of the influence of the ratio of atomizer and sheath flow and of the printing speed on printed lines. Their paper is an excellent starting point for process development.

2. Materials and methods

2.1. Optimization goals

The goal in this paper was to optimize the printing process to achieve very small feature and gap sizes down to 20 μm with a geometrical accuracy better than 5 μm. The results we found are relevant, however, as soon as feature sizes below 200 μm with a dimensional accuracy better than 20 μm is required. We were able to identify several mechanisms that can deteriorate the print quality. Through the understanding of their causes, we will suggest solutions to each of them. We want to point out that most of our observations only apply to ultra-small feature printing and could be ignored for large feature manufacturing since they usually do not require the same dimensional accuracy.

2.2. Experimental setup

An AJ5X printer by Optomec has been used for all experiment presented in the following sections. It has been loaded with the JS-221AE silver nanoparticle ink by Novacentrix in an ultrasonic cartridge and used in the three-axis setup. All experiments have been carried out with a 100 μm nozzle because it enables printing line widths as small as 10 μm. All measurements of dimensions have been taken with an optical microscope.

2.3. Generality of the results

AJ printing results are strongly dependent on the ink and substrate used as well as on all other printing parameters. Consequently, our findings on the influence of the divert/boost shutter and on crack formation are also dependent on the ink used in our experiments. The underlying principles that will be discussed in those sections apply to a wide range of inks, nonetheless. The results presented in the sections about the printing speed and about SOTF are only dependent on the machine and not on the utilized materials. They can hence directly be applied to other inks as well.

3. Results and discussion

3.1. Printing speed

Secor [13] and Mahajan *et al* [15] have demonstrated in their work, that the printing speed mainly affects the print thickness and not the line width. They have also included comprehensive theoretical explanations. When printing very small-scale structures with high precision, the printing speed exhibits another influence. In this regime, single-digit micron deviations from the desired printing path become relevant and potentially intolerable. Unfortunately, printing small structures at a high speed causes visible deformations. To demonstrate this behavior, we printed a simple rectangular pattern with speeds from 0.5 mm s^{-1} to 7 mm s^{-1} and varied the side length from 100 μm to 400 μm. The pattern and its deformation can be seen in figure 2(e): The actually printed dimension of the rectangle is smaller than the desired value. We call this error $d - d'$ the dimensional shrinkage. Additionally, some corners become rounded. This is called the corner deviation within this paper. Note that dimensional shrinkage only occurs for the axis that is performing a forth and back movement. In the example displayed here, this is the y-axis. The dimensional shrinkage can hence be seen in the height of the rectangular pattern. If the pattern was rotated by 90°, the x-axis would perform a forth and back movement resulting in a dimensional shrinkage between the left and right lines of the pattern. We measured the dimensional shrinkage for various desired side lengths and show it as dashed lines in figure 2(f). The solid lines describe the corner deformation as defined in figure 2(e). It can be seen that the errors become negligible for dimensions exceeding 400 μm and that structure sizes of 100 μm and below require printing speeds as low as 0.5 mm s^{-1} to keep the errors at bay. This limitation means that the printing speed cannot be used as a variable to control the material thickness for ultra-small structures. Instead, the atomizer flow rate and ink composition have to be utilized for this purpose.

3.2. Influence of the divert/boost shutter

We have discussed in the previous section that very small structures require a low printing speed to maintain a high dimensional accuracy. Thick printouts are the necessary result of slow printing speeds. We will discuss in the section about crack formation and prevention that a high layer thickness can lead to cracks while drying. Hence, it is desirable to limit the mass output by selecting a very low atomizer gas flow of around 10–15 standard cubic centimeters per minute. In this case, the divert/boost shutter has a noticeable influence on the printed material. To demonstrate this behavior, we turned the divert/boost shutter off for multiple minutes, and then printed the

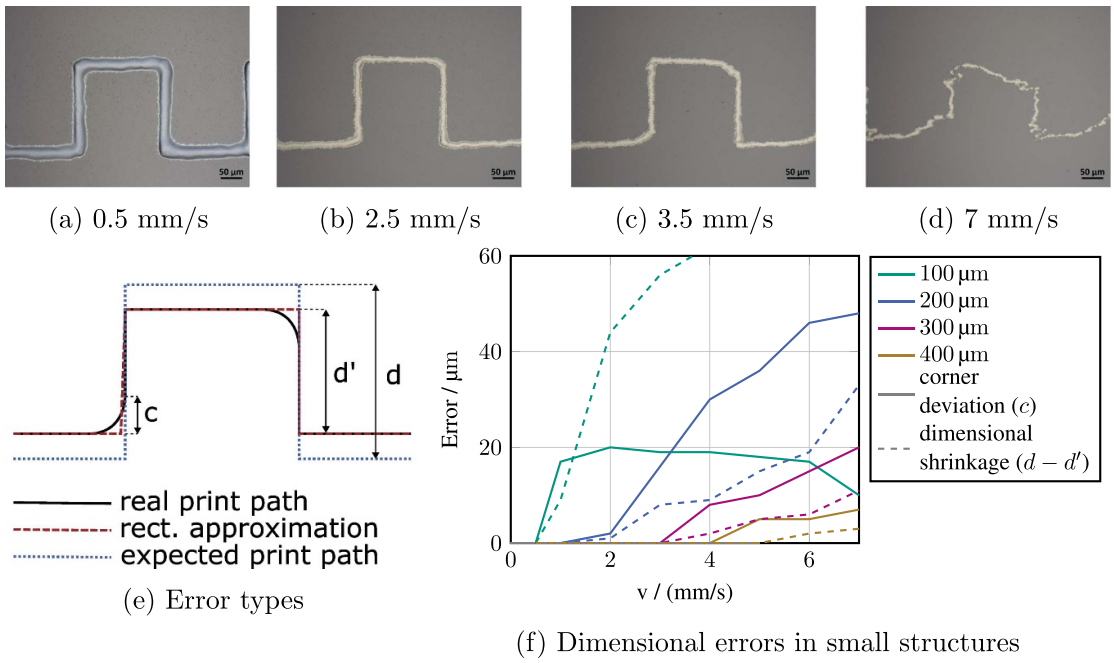

(a) 0.5 mm/s (b) 2.5 mm/s (c) 3.5 mm/s (d) 7 mm/s

(e) Error types

(f) Dimensional errors in small structures

Figure 2. Selecting a too high printing speed can cause deformations in small structures. Printed paths and their deformation for printing speeds 0.5 mm s^{-1}, 2.5 mm s^{-1}, 3.5 mm s^{-1}, 7 mm s^{-1} are shown in a, b, c and d, respectively. Figure (e) illustrates the types of errors to be expected. The dotted blue line is the programmed print path, the black line is the actually observed print path and the dashed red line is a rectangular approximation of the observed path. We call $d - d'$ the dimensional shrinkage and c the corner deviation. Figure (f) shows measurements of both errors dependent on the printing speed and on the side length d of a rectangular pattern. Solid lines depict the corner deviation and dashed lines show the dimensional shrinkage.

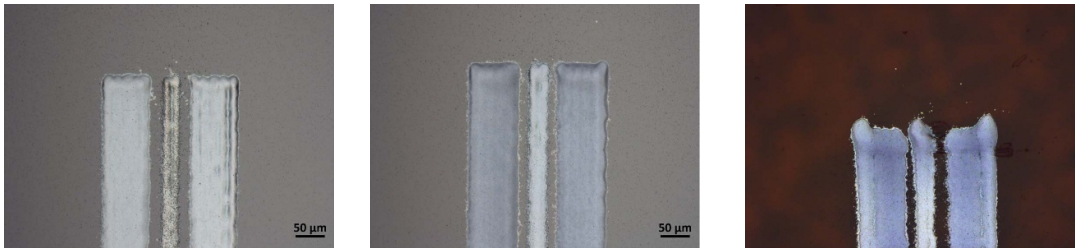

(a) 1st printed structure using divert/boost shutter (b) 5th printed structure using divert/boost shutter (c) Using the mechanical shutter only

Figure 3. The divert/boost shutter causes changing printing behavior over time in the beginning of a printout after a prolonged non-printing period, as seen in (a) and (b). Using the mechanical shutter solves this problem but causes excessive material buildup in the beginning of a print path due to the very fast reaction time and limited printer acceleration. This behavior is shown in subfigure (c) where the left and center structure show a bulge on the top left and the right structure shows a bulge on the top right corner. Those are the respective start points of the printing paths.

same test structure five times directly after each other. The result is shown in figure 3. Figure 3(a) shows the first printout after staying idle and figure 3(b) shows the fifth printout. It can be seen that the result is a more homogeneous structure which means that the printing behavior is not constant directly after turning the divert/boost shutter off for a prolonged time. Unfortunately, turning the shutter off for multiple minutes cannot be avoided in many situations because substrates need to be placed, alignment markers need to be found, etc. Small structures often have a short printing time so that a significant percentage of the print is performed in the phase of non-constant printing behavior, which reduces the reproducibility of the results. A possible solution could be to define a dumpsite that the printer goes to before every printout.

A more reliable and consistent solution would be to reduce the use of the divert/boost shutter and combine it with the mechanical shutter: The divert/boost shutter is only used for prolonged non-printing periods to prevent the mechanical shutter spoon from filling up. Shortly before the print starts and during the print, only the mechanical shutter is used to

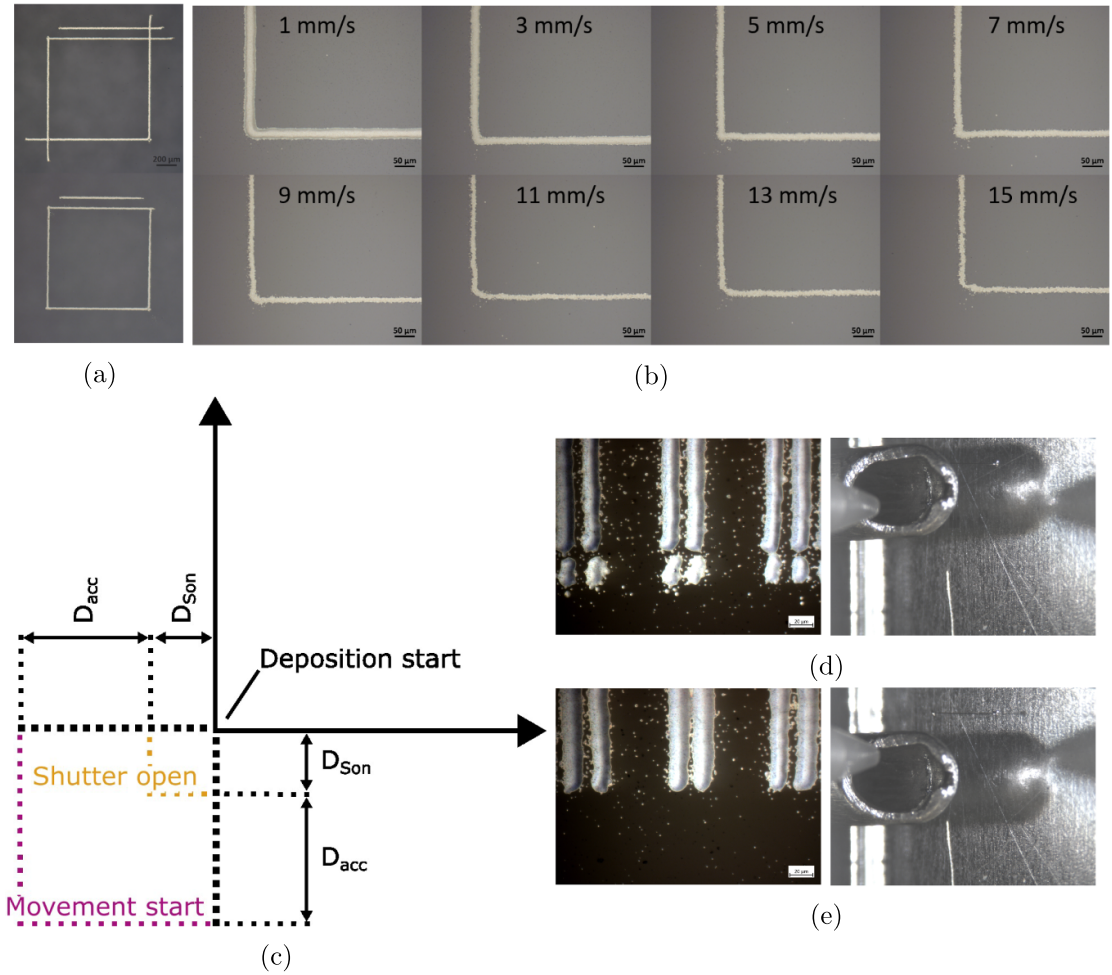

Figure 4. (a) A non-optimized shutter on the fly (SOTF) calculation routine causes long lead-in lines (top) in the SOTF test structure (bottom), which is composed of four individually printed lines forming a square and one base line. (b) The optimized SOTF subroutine code eliminates the undesired lead-in lines completely. (c) Schematic working principle of SOTF. The movement starts at the purple position. When the printer reaches the orange 'shutter open' position, it is moving already at the desired printing speed and opens the shutter. Due to the shutter open time, the printed line only starts D_{Son} later. (d) Positioning the spoon too far to the back of the printer causes undesired ink splashes at the line ends. (e) Correctly positioning the spoon eliminates them.

avoid the influence of the divert/boost shutter. This approach has been used for the print in figure 3(c). The influence from the divert/boost shutter has effectively been removed but another aggravating effect can be observed: The response time of the mechanical shutter is extremely fast—around 5 ms—which makes the acceleration of the printer visible. In the positions where the printing paths start (the corners) an excessive material buildup can be observed because the mass output is constant but the velocity is not. The remedy for this problem is using SOTF, which will be discussed in the next section.

3.3. SOTF

SOTF is a special option for the printing path creation offered by Optomec for its AJ printers. The idea is shown in figure 4(c): The movement starts with the shutter closed and it is only opened when the printhead is already accelerated to the desired printing speed. In the same way, the shutter is turned off again while the printer is still moving at the desired speed and the deceleration is done in a non-printing movement. This approach allows to remove acceleration and deceleration effects from the printed lines. There are two crucial requirements for this mode of operations: First, that the on/off timing of the shutter is well known. Second, that it is constant. Both are required to calculate the positions at which the shutter needs to be operated. Unfortunately, the default code produces the result shown in figure 4(a): there are long lead-in lines attached to the desired structures, which indicates that the calculation of the shutter open position is flawed. By performing a series of tests, we were able to exclude the shutter timing and the assumed values for the acceleration and jerk of the printer as culprits and found an imprecision in the

SOTF calculation subroutine as the error source. This subroutine calculates the position where the shutter needs to be turned on and the position where the movement starts in dependence of the desired printing velocity and the first line to be printed. We implemented an improved SOTF calculation subroutine, that reduces the complexity of the calculations and is more error resistant since we only require approximate knowledge of the printer acceleration and jerk. We ensure that the distance D_{acc} is long enough for the printer to be moving at the desired printing velocity at the shutter open position. The distance of this position to the first printed point, D_{Son}, can then be calculated with a simple motion equation:

$$D_{acc} = 0.5 \cdot a \cdot v_{print}/j + 0.5 \cdot v_{print}^2/a \quad (1)$$

$$D_{Son} = v_{print} \cdot t_{Son}, \quad (2)$$

where a is the acceleration, and j is the jerk of the printer, v_{print} is the desired printing velocity, and t_{Son} is the opening time of the shutter. Taking into account the angle of the first printed line, the x and y coordinates of the start point of the movement and of the actuation point of the shutter can be calculated. The resulting code for the ACS motion controller used in the AJ5X printer is given in the appendix. Note that only the code for the calculation of the start point is shown there, because the calculation of the shutter-off point has not been changed and this part of the code is proprietary to Optomec. We found through experiments that acceleration distances below 300 μm always cause defects even though they should theoretically be sufficient for a very low printing speed. This might be caused by higher order derivatives of the position that are not accounted for in the calculation or by delays stemming from the motion controller. However, it is simple to avoid this problem with an if-clause that ensures a minimum D_{acc}.

We ran thorough tests of our code using the mechanical shutter and the test structure shown in figure 4(a) in the bottom. The square is composed of four individually printed lines which allows to see any deficiency of the sotf routine in the corners where the lines would either not touch or form a cross if anything was off. We then swept the printing speed over a range from 1 mm s^{-1} to 15 mm s^{-1} and found the improved SOTF calculation subroutine to work perfectly for the entire range as can be seen in figure 4(b). This figure shows a zoom into the corner where both lines start. It can be seen that there is neither a gap nor a cross for any tested speed.

The movement of the mechanical shutter spoon is very fast and the system is designed in a way that allows minor vibrations. This means that the spoon must not be centered around the printing nozzle but placed more towards the front of the printer in the off-position. This placement avoids a short reopening of the shutter because of vibrations when the shutter is turned off. The effect of an improperly placed spoon is depicted in figure 4(d) and the correct placement is shown in figure 4(e). This consideration is only relevant for very small printed features and could be ignored for large lines since the distance and size of this effect would be insignificant compared to the line width.

3.4. Crack formation and prevention

During evaporation-based drying of colloidal films, a drying front can be observed that moves from the edges to the center. This process causes a buildup of capillary pressure which puts a tensile stress oriented orthogonally to the drying front on the film. It is relieved through cracks, that can be frequently observed in drying processes [16]. Those defects only occur in films with a height above a critical thickness, that depends on particle size, rigidity and packing [17]. The commonly used silver nanoparticle inks for AJ printing form a colloidal film after printing and before sintering. If the printed structures exceed a critical thickness, capillary pressure buildup during evaporation-based drying causes cracks in AJ printed silver [18]. Since nanoparticles are by definition very small (around 35 nm for the ink used in this study), the critical thickness is small as well and can be exceeded during printing. It was shown in the section about the printing speed that ultrafine features require a slow printing speed which results in a higher material thickness. This can make it impossible to stay below the critical thickness for some applications which compellingly causes cracks if the film is allowed to dry completely before sintering. If sintering starts before the film is fully dried on the other hand, sintering necks emerge that increase the particle to particle bonding significantly above the previously predominant van der Waals force. They can resist the capillary pressure and thereby prevent cracks. We submit two common causes for drying and hence cracks in AJ printing. One stems directly from the creation of the printing paths. In many scenarios it is tempting to start a job and perform other tasks while the printer is running, especially since large prints with fine features require a low printing speed and hence consume a considerable amount of time. In the end of a print, the printer stays in the last position and turns off the divert/boost shutter. Consequently, a constant stream of dry nitrogen leaves the nozzle, flows over the printed structure and dries it. Manually adding a movement command to the end of the printer script file that moves the printhead away from the printout solves this problem. The second relevant mechanism appears when the prints are thermally sintered in a non-preheated

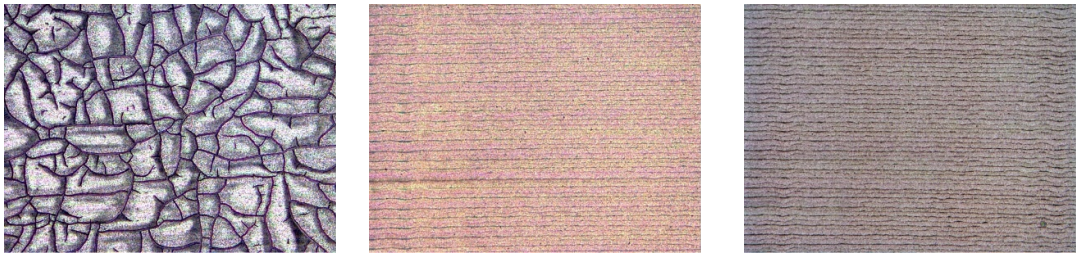

(a) Silver ink sintered on a non-preheated hotplate (b) Sintering on a preheated hotplate can avoid cracks (c) Photonic sintering can avoid cracks as well

Figure 5. Three printed silver surfaces. The crack formation in (a) is caused by drying the ink before sintering it as it happens when using a non-preheated hotplate. Using a preheated hotplate or photonic sintering can avoid this effect.

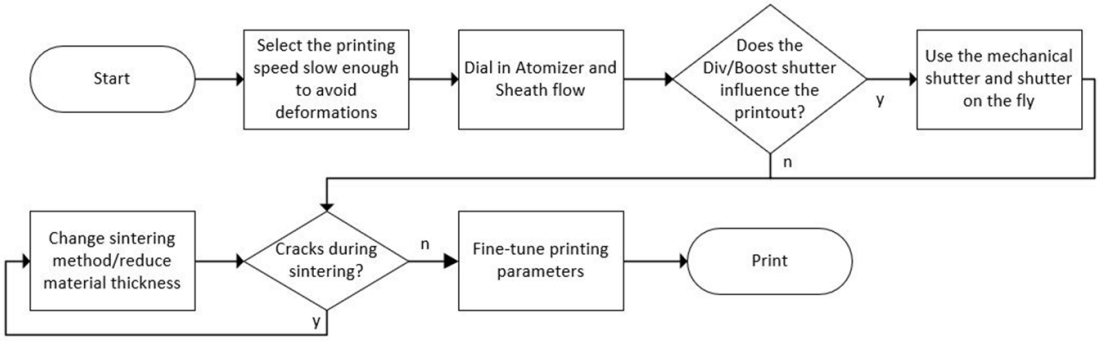

Figure 6. We suggest following this flow-chart to develop a process for ultra-fine feature AJ printing: Start with the printing speed, select the shutter mechanism, potentially fix the sintering or curing process and finally fine-tune the printing parameters.

oven or hotplate. Before a sufficiently high temperature for the formation of sintering necks is reached, the solvent left in the ink can evaporate and the printout dries. Using a preheated oven or hotplate or photonic sintering can solve this issue. Figure 5 shows cracks caused by sintering on a non-preheated hotplate and the exact same structure sintered on a preheated hotplate and a Novacentrix PulseForge 1200 photonic sintering machine. Both of them effectively avoid cracks.

The observations made in this section are heavily dependent on the utilized ink. The physical principle of crack formation in drying colloidal films is not, on the other hand. The ink only influences the critical thickness. We have presented two approaches, that can work for many applications but that do not claim generality. Every material and project requires its idiosyncratic solutions but it can be very helpful to understand that cracks can be caused by drying the ink and not only by sintering.

4. Conclusion

Printing features below 200 μm and down to 10 μm with an accuracy better than 20 μm means bringing an AJ printer to its limits. Considerations and effects become important that can be neglected in other regimes of operation. We showed that the printing speed needs to be chosen according to the geometrical accuracy requirement of the design. Unlike for printing large structures, the printing speed cannot be used to control the print thickness. This is why a very low atomizer gas flow needs to be used to limit the material thickness. We demonstrated that the divert/boost shutter can cause a non-constant printing behavior after a significant off-time. We found that using the mechanical shutter and SOTF is an excellent remedy for many problems, because it removes the influence of the divert/boost shutter and acceleration effects. We improved the SOTF calculation subroutine and included a thorough test over a wide range of printing speeds which shows that our calculation approach is indeed robust and yields an extremely high precision. We also discussed the importance of the shutter spoon placement to avoid satellite lines. Finally, we showed that drying the ink can cause cracks and suggested two sintering procedures that can avoid them. Altogether, we presented a wide range of potential pitfalls for printing ultra-small and highly precise structures with an AJ printer. For each of those potential difficulties we presented a solution. We summarized the considerations that need to be kept in mind for

ultra-fine feature and highly precise AJ printing in the flow-chart in figure 6. We hope that this work can serve as a guide to small scale AJ printing and will enable other researchers to achieve good results in less time.

Data availability statement

All data that support the findings of this study are included within the article (and any supplementary files).

Acknowledgments

This work is supported in part by BMBF within the funding for the programme Forschungslabore Mikroelektronik Deutschland (ForLab) under the reference 16ES0948.

Conflict of interest

The authors declare that they have no conflict of interest.

Appendix

Listing 1. Main program using shutter on the fly.

```
REAL XSON,YSON     ! The calculated postion in which
 ! the shutter action should start
REAL STOPEN ! The amount of time that the
 ! shutter needs for opening
REAL XFP,YFP          ! The first point of the
 ! movement; non-printing
REAL XFPP,YFPP       ! The first point of a PRINTED line
REAL XSPP,YSPP       ! The second point of a PRINTED line
 ! – used to calculate the angle of
 ! the line

STOPEN=0.003      ! Time to OPEN shutter in seconds


XFPP=0.0; YFPP=0.0; XSPP = 0.0; YSPP=1.0
Call LEAD_CALC
PTP/E (X,Y) ,XFP,YFP
XSEG(X,Y) ,XFP,YFP
LINE (X,Y) ,XSON,YSON
LINE/O (X,Y) ,XFPP,YFPP,
SetOutputsVal ,OUT,0 ,OutputsMask
LINE (X,Y) ,XSOFF,YSOFF
LINE/O (X,Y) ,XLPP,YLPP,
ResetOutputsVal ,OUT,0 ,OutputsMask
LINE (X,Y) ,XLP,YLP
ENDS (X,Y)
TILL (^X_AST.#MOVE) & (^Y_AST.#MOVE)

STOP
```

Listing 2. Shutter on the fly lead in calculations.

```
!!!!!!!!!!!!!!!!!!!!!!!!!!!!!!!!!!!!!!!!!!!!!!!!!!!!
!! Begin Shutter On The Fly Lead In Calculations !!
!!!!!!!!!!!!!!!!!!!!!!!!!!!!!!!!!!!!!!!!!!!!!!!!!!!!

GLOBAL REAL LIN_DIST

LEAD_CALC:
        ! Calculate lead in distance
        LIN_DIST = 1/2 * ACC(X) * VEL(X) / JERK(X)
        + 1/2 * POW(VEL(X) ,2) / ACC(X)

        SON_DIST = VEL(X) * STOPEN

        IF LIN_DIST < 0.300
            LIN_DIST = 0.300
        END

        ! Calculate the angle of the lead in vector
        THETA = ATAN2((YSPP – YFPP), (XSPP – XFPP))

        ! Set the lead in start positions
        XFP = XFPP – (LIN_DIST + SON_DIST) * COS(THETA)
        YFP = YFPP – (LIN_DIST + SON_DIST) * SIN(THETA)

        ! Set the shutter on positions
        XSON = XFPP – SON_DIST * COS(THETA)
        YSON = YFPP – SON_DIST * SIN(THETA)
RET
```

ORCID iDs

Georg Gramlich https://orcid.org/0009-0005-9731-3648
Robert Huber https://orcid.org/0000-0002-7457-1688

References

[1] Parate K, Rangnekar S V, Jing D, Mendivelso-Perez D L, Ding S, Secor E B, Smith E A, Hostetter J M, Hersam M C and Claussen J C 2020 Aerosol-jet-printed graphene immunosensor for label-free cytokine monitoring in serum *ACS Appl. Mater. Interfaces* **12** 8592–603
[2] Pola C C *et al* 2022 Aerosol-jet-printed graphene electrochemical immunosensors for rapid and label-free detection of SARS-CoV-2 in saliva *2D Mater.* **9** 035016
[3] Yang C, Zhou E, Miyanishi S, Hashimoto K and Tajima K 2011 Preparation of active layers in polymer solar cells by aerosol jet printing *ACS Appl. Mater. Interfaces* **3** 4053–8
[4] Lu S, Cardenas J A, Worsley R, Williams N X, Andrews J B, Casiraghi C and Franklin A D 2019 Flexible, print-in-place 1D-2D thin-film transistors using aerosol jet printing *ACS Nano* **13** 11263–72
[5] Craton M T, Konstantinou X, Albrecht J D, Chahal P and Papapolymerou J 2020 A chip-first microwave package using multimaterial aerosol jet printing *IEEE Trans. Microw. Theory Tech.* **68** 3418–27
[6] Oakley C, Albrecht J D, Papapolymerou J and Chahal P 2019 Low-loss aerosol-jet printed wideband interconnects for embedded devices *IEEE Trans. Compon. Packag. Manuf. Technol.* **9** 2305–13
[7] Xaver Röhrl F, Jakob J, Bogner W, Weigel R and Zorn S 2018 *Bare Die Connections via Aerosol Jet Technology for Millimeter Wave Applications* (IEEE)
[8] Craton M T, Albrecht J D, Chahal P and Papapolymerou J 2021 Additive manufacturing of a wideband capable *W* -band packaging strategy *IEEE Microw. Wirel. Compon. Lett.* **31** 697–700
[9] Ihle M, Ziesche S, Zech C and Baumann B 2019 Functional printing of MMIC-interconnects on LTCC packages for sub-THz applications *22nd European Microelectronics and Packaging Conf. & Exhibition (EMPC) (Italy, 16–19 September 2019)* (https://doi.org/10.23919/EMPC44848.2019.8951799)
[10] Gramlich G, Hebeler J, Bohn C, Lemmer U and Zwick T 2022 Aerosol jet printed microstrip lines on polyimide for d-band *European Microwave Conf. (EuMC) (United Kingdom, 04–6 April 2022)* (https://doi.org/10.23919/EuMC50147.2022.9784303)
[11] Gramlich G, Huber R, Lemmer U and Zwick T 2022 Aerosol jet printed millimeter wave interconnects in d-band *European Microwave Conf. (EuMC) (Italy, 27–29 September 2022)* (https://doi.org/10.23919/EuMC54642.2022.9924311)
[12] Wilkinson N J, Smith M A A, Kay R W and Harris R A 2019 A review of aerosol jet printing—a non-traditional hybrid process for micro-manufacturing *Int. J. Adv. Manuf. Technol.* **105** 4599–619
[13] Secor E B 2018 Principles of aerosol jet printing *Flex. Print. Electron.* **3** 035002
[14] Feng J Q, Ramm A and Renn M J 2021 A quantitative analysis of overspray in aerosol jet® printing *Flex. Print. Electron.* **6** 045006
[15] Mahajan A, Daniel Frisbie C and Francis L F 2013 Optimization of aerosol jet printing for high-resolution, high-aspect ratio silver lines *ACS Appl. Mater. Interfaces* **5** 4856–64
[16] Tirumkudulu M S and Russel W B 2005 Cracking in drying latex films *Langmuir* **21** 4938–48
[17] Singh K B and Tirumkudulu M S 2007 Cracking in drying colloidal films *Phys. Rev. Lett.* **98** 218302
[18] Dalal N, Gu Y, Hines D R, Dasgupta A and Das S 2019 Cracks in the 3D-printed conductive traces of silver nanoparticle ink *J. Micromech. Microeng.* **29** 097001